



## Precision predictions for supersymmetric dark matter

J. Harz

*Department of Physics and Astronomy, University College London, London WC1E 6BT, United Kingdom*

B. Herrmann

*LAPTh, Université de Savoie, CNRS, 9 Chemin de Bellevue, B.P. 110, 74941 Annecy-le-Vieux, France*

M. Klasen, K. Kovarik, M. Meinecke, P. Steppeler

*Institut für Theoretische Physik, Westfälische Wilhelms-Universität Münster, Wilhelm-Klemm-Straße 9, 48149 Münster, Germany*

---

### Abstract

The dark matter relic density has been measured by Planck and its predecessors with an accuracy of about 2%. We present theoretical calculations with the numerical program DM@NLO in next-to-leading order SUSY QCD and beyond, which allow to reach this precision for gaugino and squark (co-)annihilations, and use them to scan the phenomenological MSSM for viable regions, applying also low-energy, electroweak and hadron collider constraints.

*Keywords:*

Dark Matter, Supersymmetry, QCD

---

### 1. Introduction

Today, there is ample evidence for the existence of Cold Dark Matter (CDM) in the Universe from many different scales, ranging from rotational velocity curves of galaxies and galaxy clusters to gravitational lensing, structure formation and the cosmic microwave background. Through a six-parameter fit to a standard, spatially flat  $\Lambda$ CDM cosmological model, the Planck mission has determined the relic density of the CDM, with an accuracy of about 2%, to be [1]

$$\Omega_{\text{CDM}} = 0.1199 \pm 0.0027. \quad (1)$$

Since the Standard Model (SM) of particle physics contains no weakly-interacting, sufficiently massive particle, this measured value and its uncertainty highly constrain all SM extensions that could provide a viable dark matter candidate. Among these extensions, the Minimal Supersymmetric SM (MSSM) has by far received the most attention, in particular the lightest neutralino ( $\tilde{\chi}_1^0$ ) stabilised by a discrete ( $R$ ) symmetry.

Supersymmetry (SUSY) is attractive for many theoretical and phenomenological reasons. Not only does it relate the two fundamentally different types of particles, fermions and bosons, through SUSY partners, which otherwise share the same quantum numbers, but also it represents the maximal possible extension of space-time symmetry (the Poincaré algebra). In addition, the SUSY partners change the  $\beta$  functions and thus the running of couplings and masses, making (in contrast to the SM alone) Grand Unified Theories (GUTs) phenomenologically viable. Last, but not least, the mass of the lightest, SM-like Higgs boson  $m_{h^0}$  is stabilised, in particular through the contributions of light top squarks  $\tilde{t}$ , which provide a crucial second term in the relation

$$m_{h^0}^2 = m_Z^2 \cos^2 2\beta + \frac{3g^2 m_t^4}{8\pi^2 m_W^2} \left[ \log \frac{M_{\text{SUSY}}^2}{m_t^2} + \frac{X_t^2}{M_{\text{SUSY}}^2} \left( 1 - \frac{X_t^2}{12M_{\text{SUSY}}^2} \right) \right]. \quad (2)$$

Here,  $X_t = A_t - \mu/\tan\beta$  and  $M_{\text{SUSY}} = \sqrt{m_{\tilde{t}_1} m_{\tilde{t}_2}}$  control the mixing in the stop sector, which must be nearly maximal ( $|X_t| = \sqrt{6} M_{\text{SUSY}}$ ), with large  $A_t$  and a light stop  $\tilde{t}_1$ , to explain the relatively high observed Higgs boson mass of  $125.36 \pm 0.37(\text{stat.}) \pm 0.18(\text{syst.})$  GeV [2] and  $125.03^{+0.26}_{-0.27}(\text{stat.})^{+0.13}_{-0.15}(\text{syst.})$  GeV [3], respectively. Since SUSY spectrum generators such as SPheno [4] have relatively large theoretical uncertainties, one usually relaxes the Higgs mass constraint, e.g. to  $122 \text{ GeV} \leq m_{h^0} \leq 128 \text{ GeV}$ . Other important constraints on the MSSM model parameters come from loop contributions in rare  $B$  meson decays, in particular  $2.77 \cdot 10^{-4} \leq \text{BR}(b \rightarrow s\gamma) \leq 4.33 \cdot 10^{-4}$  at  $3\sigma$  [5], and from direct SUSY particle searches at the LHC, with null results in particular for gluinos and first and second generation squarks with masses below about 1 TeV [6, 7]. Currently less important are constraints from the anomalous magnetic moment of the muon and electroweak precision measurements at LEP.

All of these constraints are applied in our random scans of a phenomenologically motivated subset of eight MSSM parameters at the TeV scale (pMSSM-8), e.g.

$$\begin{aligned}
 500 \text{ GeV} &\leq M_{\tilde{q}_{1,2}} \leq 4000 \text{ GeV}, \\
 100 \text{ GeV} &\leq M_{\tilde{q}_3} \leq 2500 \text{ GeV}, \\
 500 \text{ GeV} &\leq M_{\tilde{t}} \leq 4000 \text{ GeV}, \\
 |T_t| &\leq 5000 \text{ GeV}, \\
 200 \text{ GeV} &\leq M_1 \leq 1000 \text{ GeV}, \\
 100 \text{ GeV} &\leq m_A \leq 2000 \text{ GeV}, \\
 |\mu| &\leq 3000 \text{ GeV}, \\
 2 \leq \tan\beta &\leq 50.
 \end{aligned} \tag{3}$$

In addition, the GUT relations for  $M_{2,3}$  can be relaxed, as can be the parameter  $M_{\tilde{u}_3}$ , leading to eleven free parameters (pMSSM-11).

## 2. Neutralino/chargedino coannihilation

Apart from the annihilation of the CDM particle, the lightest neutralino  $\tilde{\chi}_1^0$ , with itself, many co-annihilation processes can become relevant or even dominant in different regions of the pMSSM. These processes may in particular be co-annihilations between different types of neutral gauginos and higgsinos (neutralinos) and charged gauginos and higgsinos (charginos), as shown at the tree-level in Fig. 1. At this level, all of these processes are routinely included in programs such as micrOMEGAs [8] and DarkSUSY [9]. They become rele-

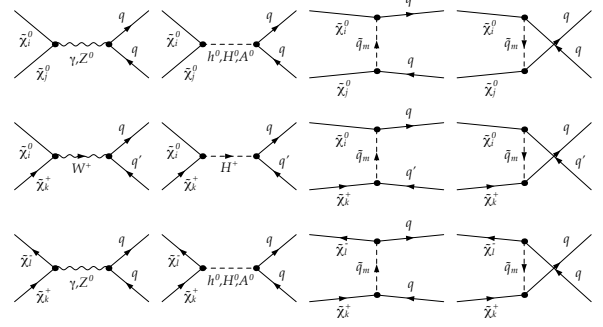


Figure 1: Tree level diagrams of the gaugino (co-)annihilation processes  $\tilde{\chi}_i^0 \tilde{\chi}_j^0 \rightarrow q\bar{q}$  (top),  $\tilde{\chi}_i^0 \tilde{\chi}_k^\pm \rightarrow q\bar{q}'$  (middle), and  $\tilde{\chi}_k^\pm \tilde{\chi}_l^\pm \rightarrow q\bar{q}$  (bottom).

vant, when the ratios of equilibrium densities

$$\frac{n_i^{\text{eq.}}}{n_j^{\text{eq.}}} \sim \exp\left\{-\frac{m_i - m_j}{T}\right\} \tag{4}$$

are only weakly Boltzmann suppressed, i.e. when the mass differences of the SUSY particles  $i$  and  $j$  are small. For three different reference scenarios [10], the most relevant gaugino (co-)annihilation contributions into quarks are shown in Tab. 1.

After generalising these processes to allow for general types of flavour violation [11, 12, 13, 14], we have now computed all their SUSY-QCD corrections and implemented these in a numerical code named DM@NLO (<http://dmnlo.hepforge.org>) [10]. This includes previously calculated corrections to the annihilation of two lightest neutralinos into heavy quarks through the Higgs funnel  $\tilde{\chi}_1^0 \tilde{\chi}_1^0 \rightarrow A^0 \rightarrow b\bar{b}$  [15], other Higgs resonances [16], or gauge boson and squark exchanges with bottom and top quark final states [17]. New in our recent work is not only the generalisation of the initial state, but also the generalisation of the final state to first and second generation quarks, which are in general not negligible as one can see from Tab. 1.

Typical one-loop diagrams are depicted in Fig. 2, real emission diagrams in Fig. 3. Among them, the infrared poles cancel, while the ultraviolet ones occurring in the one-loop diagrams are removed by renormalisation (for details see Ref. [19]). The infrared poles in the real corrections are made explicit and the finite remainder is treated numerically with the Catani-Seymour dipole subtraction method [18],

$$\sigma_{\text{NLO}} = \int_3 \left[ d\sigma^{\text{R}} \Big|_{\epsilon=0} - d\sigma^{\text{A}} \Big|_{\epsilon=0} \right] + \int_2 \left[ d\sigma^{\text{V}} + \int_1 d\sigma^{\text{A}} \right]_{\epsilon=0}. \tag{5}$$

After imposing the relic density constraint, the numerical impact of the corrections on the viable param-

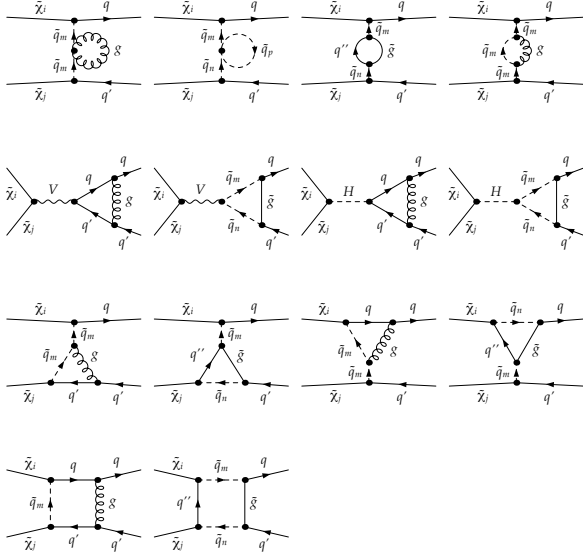


Figure 2: Diagrams depicting schematically the one-loop corrections of  $\mathcal{O}(\alpha_s)$  to the gaugino (co-)annihilation processes shown in Fig. 1. Here,  $V = \gamma, Z^0, W^\pm$  and  $H = h^0, H^0, A^0, H^\pm$ . The corrections to the  $u$ -channel processes are not explicitly shown, as they can be obtained by crossing from the corresponding  $t$ -channel diagrams.

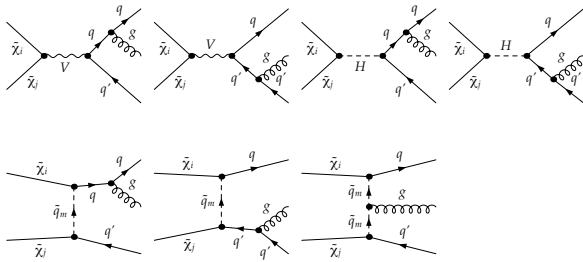


Figure 3: Diagrams depicting the real gluon emission corrections of  $\mathcal{O}(\alpha_s)$  to the gaugino (co-)annihilation processes shown in Fig. 1. As before,  $V = \gamma, Z^0, W^\pm$  and  $H = h^0, H^0, A^0, H^\pm$ . The corrections to the  $u$ -channel processes are not explicitly shown, as they can be obtained by crossing from the corresponding  $t$ -channel diagrams.

Table 1: Most relevant gaugino (co-)annihilation channels into quarks in three typical pMSSM-11 scenarios [10]. Channels which contribute less than 0.1% to the thermally averaged cross section are not shown.

	Scen. I	Scen. II	Scen. III
$\tilde{\chi}_1^0 \tilde{\chi}_1^0 \rightarrow t\bar{t}$	1.4%	15.0%	–
$b\bar{b}$	9.1%	5.9%	–
$c\bar{c}$	–	0.1%	–
$u\bar{u}$	–	0.1%	–
$\tilde{\chi}_1^0 \tilde{\chi}_2^0 \rightarrow t\bar{t}$	2.5%	12.0%	3.3%
$b\bar{b}$	23.0%	6.9%	1.6%
$c\bar{c}$	–	–	1.3%
$s\bar{s}$	–	–	1.7%
$u\bar{u}$	–	–	1.3%
$d\bar{d}$	–	–	1.7%
$\tilde{\chi}_1^0 \tilde{\chi}_3^0 \rightarrow t\bar{t}$	–	9.1%	–
$b\bar{b}$	–	5.3%	–
$\tilde{\chi}_2^0 \tilde{\chi}_2^0 \rightarrow b\bar{b}$	0.2%	–	–
$\tilde{\chi}_1^0 \tilde{\chi}_1^\pm \rightarrow t\bar{b}$	43.0%	40.0%	0.8%
$c\bar{s}$	–	–	8.5%
$u\bar{d}$	–	–	8.5%
$\tilde{\chi}_2^\pm \tilde{\chi}_1^\pm \rightarrow t\bar{b}$	0.4%	–	0.4%
$c\bar{s}$	0.9%	–	4.6%
$u\bar{d}$	0.9%	–	4.6%
$\tilde{\chi}_1^\pm \tilde{\chi}_1^\pm \rightarrow t\bar{t}$	0.2%	–	3.2%
$b\bar{b}$	0.6%	–	2.7%
$c\bar{c}$	0.2%	–	2.3%
$s\bar{s}$	0.2%	–	1.4%
$u\bar{u}$	0.2%	–	2.3%
$d\bar{d}$	0.2%	–	1.4%
Total	83.0%	94.4%	51.6%

eter space becomes visible in Fig. 4. Here we only show the plane of gaugino mass parameters  $M_1$  and  $M_2$  and fix all other pMSSM-11 parameters. More than 70 or 80% of all contributing (co-)annihilation processes are computed at next-to-leading order (NLO) of SUSY-QCD with DM@NLO, leading to corrections to the relic density of 5% or more and a clearly visible shift of the Planck contour from tree-level (grey) to NLO (blue). The standard micrOMEGAs result, which tries to capture some corrections through effective vertices, agrees with neither prediction in this particular case.

### 3. Electroweak stop coannihilation

When the top squark mass comes close to the lightest neutralino mass, as it is natural from the arguments given in the introduction, but also for cosmological reasons, co-annihilations among these particles

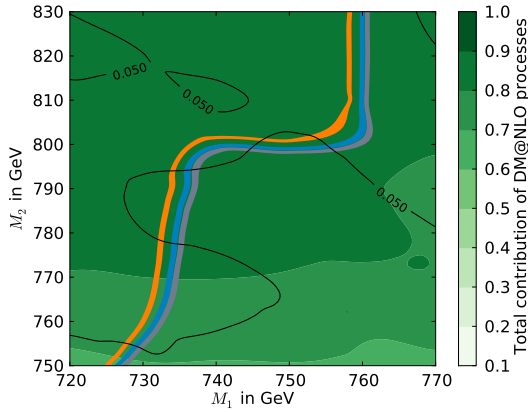


Figure 4: Neutralino relic density in the  $M_1$ – $M_2$ -plane surrounding scenario I. The three coloured lines represent the part of the parameter space which leads to a neutralino relic density compatible with the Planck limits given in Eq. (1). For the orange line we used the standard micrOMEGAs routine, the grey one corresponds to our tree level calculation, and the blue one represents our full one-loop calculation. The black contour lines denote the relative shift between the tree level and one-loop relic density, i.e.  $|1 - \Omega_\chi^{\text{NLO}}/\Omega_\chi^{\text{tree}}|$ .

may also occur, as shown at the tree level in Fig. 5. These processes must then also be corrected in a similar way as described above. This has now been achieved and implemented in DM@NLO [19, 20]. In a previously performed calculation [21], only the co-annihilation of bino-like neutralinos with right-handed stops into top quarks and gluons as well as bottom-quarks and  $W$ -bosons was considered. We have now corrected all co-annihilation processes, irrespective of the gaugino/higgsino or top squark decomposition, and included all electroweak final states (see Fig. 6). An important subtlety arises from intermediate on-shell top quarks, cf. Fig. 7. These diagrams also contribute to the elec-

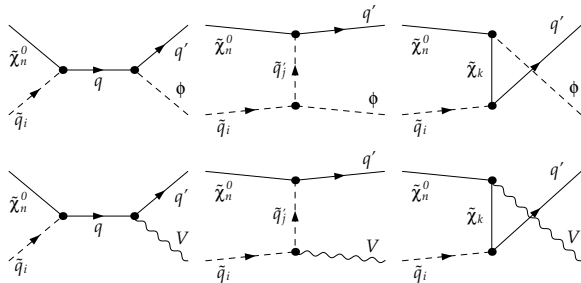


Figure 5: Leading-order Feynman diagrams for neutralino-squark co-annihilation into a quark and a Higgs boson ( $\phi = h^0, H^0, A^0, H^\pm$ ) or an electroweak gauge boson ( $V = \gamma, Z^0, W^\pm$ ). The  $u$ -channel is absent for a photon in the final state.

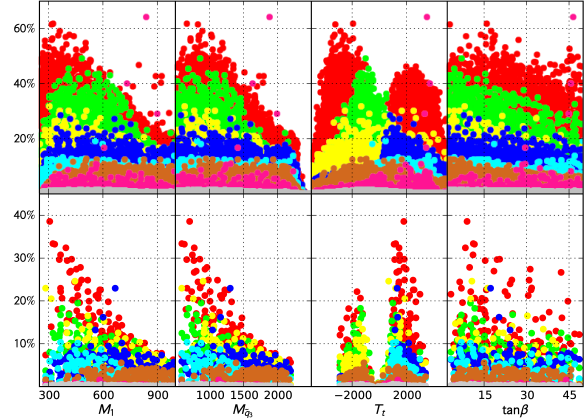


Figure 6: Relative contributions of the neutralino-stop co-annihilation channels for the generated parameter points as a function of the input parameters  $M_1$ ,  $M_{\tilde{q}_3}$ ,  $T_t$ , and  $\tan\beta$  before (top) and after (bottom) applying selection cuts. Shown are the contributions from  $t\bar{h}^0$  (red),  $t\bar{g}$  (green),  $t\bar{Z}^0$  (blue),  $t\bar{H}^0$  (yellow),  $b\bar{W}^+$  (cyan),  $t\bar{A}^0$  (chocolate),  $b\bar{H}^+$  (pink), and  $t\bar{\gamma}$  (silver) final states. The parameters  $M_1$ ,  $M_{\tilde{q}_3}$ , and  $T_t$  are given in GeV.

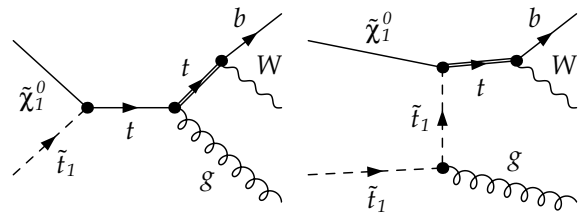


Figure 7: Real gluon emission diagrams with a  $Wb$  final state where an internal top quark can become on-shell, as indicated by a double line.

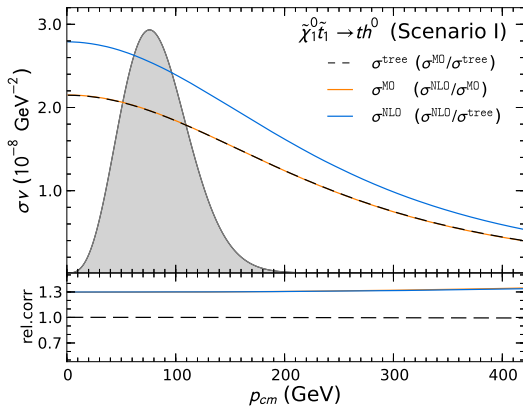


Figure 8: Tree-level (black dashed line), full one-loop (blue solid line) and *micrOMEGAs* (orange solid line) cross-section for a top-Higgs final state in a typical reference scenario. The upper part of the plot shows the absolute value of  $\sigma\nu$  together with the thermal distribution (in arbitrary units), whereas the lower part shows the corresponding relative shifts (second item in the legend).

troweak corrections of top-gluon final states. In order to avoid double counting, we subtract a local gauge-invariant term defined by the squared resonant amplitude with the top quark on shell except for the propagator denominator, which is kept as a general Breit-Wigner function

$$|\mathcal{M}_{2\rightarrow 3}^{\text{sub}}|^2 = \frac{m_t^2 \Gamma_t^2}{(p_t^2 - m_t^2)^2 + m_t^2 \Gamma_t^2} |\mathcal{M}_{2\rightarrow 3}^{\text{res}}|^2_{p_t^2 = m_t^2} \quad (6)$$

(cf. also Ref. [22]).

The numerical impact of our SUSY-QCD corrections on the velocity-weighted cross section  $\sigma\nu$  for a top-Higgs final state in a typical co-annihilation scenario can be seen in Fig. 8. In this case, the *micrOMEGAs* prediction (orange) fully agrees with our tree-level result (grey) when using the same top quark mass, while the NLO prediction (blue) is about 30% larger. The relic density is then increased by about 9%, which is comparable to the corrections obtained in the gaugino co-annihilation scenarios.

#### 4. Conclusion

To summarise, the SUSY-QCD corrections to all gaugino co-annihilation processes into light and heavy quarks as well as to gaugino-squark co-annihilations into electroweak final states have now been computed and implemented in *DM@NLO*. They amount typically to increases in the cross section of 5–30% and shifts in the

Planck relic density band that can exceed its experimental uncertainty. The effective vertex approach implemented e.g. in *micrOMEGAs* is in general not able to correctly capture the higher-order corrections, which can induce significant shifts in the extracted SUSY parameters. Our corrections are implemented using general couplings, making them generalisable to other, in particular non-supersymmetric models. Note that loop corrections and co-annihilation processes can sometimes change the picture even qualitatively, not only quantitatively, as it has been shown for inert Higgs doublet [23] and radiative seesaw models [24].

#### Acknowledgments

We thank Q. Le Boulc’h for his collaboration on the stop co-annihilation channels. The work of J.H. was supported by the London Centre for Terauniverse Studies (LCTS), using funding from the European Research Council via the Advanced Investigator Grant 267352. The group in Münster is supported by the Helmholtz Alliance for Astroparticle Physics and the Deutsche Forschungsgemeinschaft under grant KL 1266/5-1.

#### References

- [1] P. A. R. Ade *et al.* [Planck Collaboration], *Astron. Astrophys.* (2014) [arXiv:1303.5076 [astro-ph.CO]].
- [2] G. Aad *et al.* [ATLAS Collaboration], arXiv:1406.3827 [hep-ex].
- [3] CMS Collaboration [CMS Collaboration], CMS-PAS-HIG-14-009.
- [4] W. Porod and F. Staub, *Comput. Phys. Commun.* **183** (2012) 2458 [arXiv:1104.1573 [hep-ph]].
- [5] D. Asner *et al.* [Heavy Flavor Averaging Group Collaboration], arXiv:1010.1589 [hep-ex], and online update at <http://www.slac.stanford.edu/xorg/hfag>.
- [6] G. Aad *et al.* [ATLAS Collaboration], arXiv:1405.7875 [hep-ex].
- [7] S. Chatrchyan *et al.* [CMS Collaboration], *JHEP* **1406** (2014) 055 [arXiv:1402.4770 [hep-ex]].
- [8] G. Belanger, F. Boudjema, A. Pukhov and A. Semenov, *Comput. Phys. Commun.* **185** (2014) 960 [arXiv:1305.0237 [hep-ph]].
- [9] P. Gondolo, J. Edsjo, P. Ullio, L. Bergstrom, M. Schelke and E. A. Baltz, *JCAP* **0407** (2004) 008 [astro-ph/0406204].
- [10] B. Herrmann, M. Klasen, K. Kovarik, M. Meinecke and P. Steppele, *Phys. Rev. D* **89** (2014) 114012 [arXiv:1404.2931 [hep-ph]].
- [11] G. Bozzi, B. Fuks, B. Herrmann and M. Klasen, *Nucl. Phys. B* **787** (2007) 1 [arXiv:0704.1826 [hep-ph]].
- [12] B. Fuks, B. Herrmann and M. Klasen, *Nucl. Phys. B* **810** (2009) 266 [arXiv:0808.1104 [hep-ph]].
- [13] B. Fuks, B. Herrmann and M. Klasen, *Phys. Rev. D* **86** (2012) 015002 [arXiv:1112.4838 [hep-ph]].
- [14] B. Herrmann, M. Klasen and Q. Le Boulc’h, *Phys. Rev. D* **84** (2011) 095007 [arXiv:1106.6229 [hep-ph]].
- [15] B. Herrmann and M. Klasen, *Phys. Rev. D* **76** (2007) 117704 [arXiv:0709.0043 [hep-ph]].

- [16] B. Herrmann, M. Klasen and K. Kovarik, Phys. Rev. D **79** (2009) 061701 [arXiv:0901.0481 [hep-ph]].
- [17] B. Herrmann, M. Klasen and K. Kovarik, Phys. Rev. D **80** (2009) 085025 [arXiv:0907.0030 [hep-ph]].
- [18] S. Catani, S. Dittmaier, M. H. Seymour and Z. Trocsanyi, Nucl. Phys. B **627** (2002) 189 [hep-ph/0201036].
- [19] J. Harz, B. Herrmann, M. Klasen, K. Kovarik and Q. L. Boulc'h, Phys. Rev. D **87** (2013) 5, 054031 [arXiv:1212.5241].
- [20] J. Harz, B. Herrmann, M. Klasen, K. Kovarik and Q. Le Boulc'h, PoS Corfu **2012** (2013) 075 [arXiv:1302.3525 [hep-ph]].
- [21] A. Freitas, Phys. Lett. B **652** (2007) 280 [arXiv:0705.4027 [hep-ph]].
- [22] W. Beenakker, R. Hopker, M. Spira and P. M. Zerwas, Nucl. Phys. B **492** (1997) 51 [hep-ph/9610490].
- [23] M. Klasen, C. E. Yaguna and J. D. Ruiz-Alvarez, Phys. Rev. D **87** (2013) 075025 [arXiv:1302.1657 [hep-ph]].
- [24] M. Klasen, C. E. Yaguna, J. D. Ruiz-Alvarez, D. Restrepo and O. Zapata, JCAP **1304** (2013) 044 [arXiv:1302.5298 [hep-ph]].